Long streamers in the upper atmosphere above thundercloud

1998 J. Phys. D: Appl. Phys. 31 3255

(http://iopscience.iop.org/0022-3727/31/22/014)

J. Phys. D: Appl. Phys. **31** (1998) 3255–3264. Printed in the UK PII: S0022-3727(98)94154-7

Long streamers in the upper atmosphere above thundercloud

Yu P Raizer†, G M Milikh‡, M N Shneider† and S V Novakovski‡

† Institute of Problems of Mechanics, Russian Academy of Sciences,
101 Vernadsky Str., 117526 Moscow, Russia
‡ Departments of Astronomy and Physics, University of Maryland, College Park,
Maryland 20742, USA

Received 12 May 1998, in final form 1 September 1998

Abstract. It has been suggested that optical flashes observed in the upper atmosphere above giant thunderstorms (red sprites) are due to streamers. Such streamers are initiated in the lower ionosphere by electron patches caused by electromagnetic radiation from horizontal intracloud lightning and then develop downward in the static electric field due to the thundercloud. The triggering conditions of streamer development are analysed in the paper. Using similarity relations, known characteristics of streamer tips obtained earlier in laboratory conditions are extended to a description of streamers in rare air. Streamer growth in the nonuniform atmosphere is calculated. It is shown that streamers first appear at a height of about 80 km and then grow downward to slightly below 50 km, where they are terminated. This is in agreement with red sprite observations. An altitude distribution of the streamer generated plasma is obtained. The simple models of streamer development presented in this paper could be applied for computations of streamers growing in various other conditions.

1. Introduction

Recently discovered 'red sprites'—optical flashes predominantly in the red located at 50–90 km above ground and associated with giant thunderstorms—have been the focus of many recent ground and aircraft campaigns [1–3]. In fact, the most recent optical observation made with photometers of high spatial resolution revealed that red sprites start as a luminous cloud which then propagates mostly downward developing a highly branched structure [4] which resembles streamers usually observed in dense gases [5]. Current models [6–8] attribute red sprites to the heating of ambient electrons due to quasistatic (QS) electric fields or electromagnetic pulses (EMPs) from lightning. The energized electrons in turn cause ionization and optical emissions. These models, however, rely on a laminar electric field from lightning and cannot explain the observed streamer structure of red sprites.

The objective of this paper is to present a model of streamer development in the lower ionosphere caused by EMPs from lightning, as well as its downward propagation in the upper atmosphere in the thundercloud electric field. We address topics such as the triggering conditions of streamer development and how far can a streamer propagate downward. The role of the streamer nucleolus can be played by patches of enhanced ionization generated by EMPs from horizontal intracloud lightning [9]. A schematic diagram of the proposed model is given in figure 1. Aside from their relevance to lightning studies, this paper describes some peculiarities of streamer development in the rear nonuniform atmosphere.

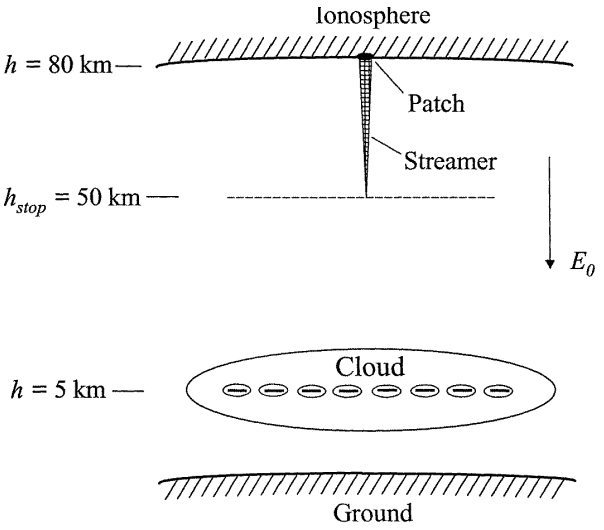

Figure 1. Schematic diagram of streamer development above thundercloud.

2. Plasma patches due to intracloud lightning

It is well known that lightning discharges follow a tortuous path [10]. It has also been shown that intracloud discharges

resemble the Lichtenberg patterns observed in dielectric breakdown [11]. A current pulse propagating along the tortuous path radiates the EMPs. The process can be considered as similar to the radiation of an array of radiators each having a given phase. If these phases are distributed according to a certain law then, in the lower ionosphere, i.e. in the far zone of the radiators, the radiation field will display maxima and minima due to the interference between different EMPs. The maxima appear where the phases from the radiators add up almost coherently, showing a significant gain over a random distribution, while the minima correspond to the phase cancellation.

To determine the extent and the distance over which ballistic effects resulting from the lightning discharge affect the power density structure projected in the upper atmosphere and lower ionosphere, a numerical model of the intracloud lightning discharge was presented [9]. In this model the intracloud lightning is taken to be a set of nonuniform distributed small current line elements. A current pulse propagates with a given speed along a dendritic structure. The radiation field is a superposition, with the respective phases, of the small line current elements that form the discharge. In the model a power law distribution in the phases is assumed. Such a model describes the spatial structure and intensity of the radiation pattern in the lower ionosphere.

Furthermore, as lightning induced fields propagate in the lower ionosphere, the field changes the properties of the medium by heating electrons which in turn ionize air molecules. The model indicates that an interference pattern from intracloud lightning generates a wide range of scales in the low ionosphere, producing patches of electron temperature and density perturbations. Such patches could serve as streamer nucleoli by acting as catalysts that drive streamers when they interact with the laminar field of the thundercloud, as described in the following.

3. QS electric field generated by lightning discharges

In this section we consider a quasistatic electric field generated in the upper atmosphere above the thundercloud. A quasineutral thundercloud consists of two layers of different charge. After one layer is removed by a cloud-to-ground discharge a vertical QS field is established in the atmosphere above the thundercloud. This field endures for a time equal to the local relaxation time $\tau_r = \epsilon_0/\sigma$, where ϵ_0 is the permittivity of vacuum and σ is the local ionospheric conductivity in the presence of the electric field. At night the QS field penetrates to altitudes $h \approx 80$ km where $\tau_r \approx 1$ ms [7].

Using a simple dipole model with cloud charge Q left at altitude z above a perfectly conducting ground, which forms an image charge located at a depth z beneath the ground, we obtain the following expression for the resulting QS electric field as a function of altitude h

$$E = \frac{Q}{4\pi\epsilon_0}\left(\frac{1}{(h-z)^2} - \frac{1}{(h+z)^2}\right). \tag{1}$$

It is known that sprites are predominantly associated with positive cloud-to-ground discharges [2]. In this case $Q < 0$, the electric field is directed downward, and the streamer is positive (cathode-directed).

An additional contribution comes from charges induced in the ionosphere. Assuming the ionosphere is a perfect conductor at an altitude h_i, the first-order correction is a vertical image dipole the centre of which is located at $2h_i$ above ground [7]. Correspondingly the total field is given by

$$E = \frac{Q}{4\pi\epsilon_0}\left[\left(\frac{1}{(h-z)^2} - \frac{1}{(h+z)^2}\right) + \left(\frac{1}{(2h_i-h-z)^2} - \frac{1}{(2h_i-h+z)^2}\right)\right]. \tag{2}$$

We consider the electric field generated in the upper atmosphere at the altitude $h \gg z$. Thus equation (2) becomes

$$E = \frac{zQ}{\pi\epsilon_0 h^3}\left[1 + \left(\frac{h}{2h_i - h}\right)^3\right]. \tag{3}$$

Considering a conducting ionosphere at $h_i \simeq 80$ km the potential of this field becomes

$$U_0 = -\varphi_0\left[\left(\frac{h_i}{h}\right)^2 - \left(\frac{h_i}{2h_i-h}\right)^2\right] \qquad \varphi_0 = \frac{z|Q|}{2\pi\epsilon_0 h_i^2}. \tag{4}$$

We chose φ_0 from the condition that at $h = h_i$ the field due to the thundercloud becomes the ionizing field, i.e. $E(h_i) \simeq 0.5$ V cm^{-1} for a corresponding air density $N = 4\times10^{14}$ cm^{-3}. In fact, if a cloud charge of 70 C is left unbalanced at the altitude $z = 5$ km it generates an electric field of 0.5 V cm^{-1} at 80 km within a microsecond after the lightning discharge. Furthermore the cloud potential $U_0(z) \simeq -240$ MV, while $\varphi_0 \simeq 0.97$ MV. Note that in the following analysis we consider a streamer initiated at the conducting surface (lower ionosphere) and propagating downward along the coordinate x such that $x = h_i - h$. Correspondingly the potential of the external source of the streamer is given by

$$U_0(x) = -\varphi_0\left[\left(\frac{h_i}{h_i-x}\right)^2 - \left(\frac{h_i}{h_i+x}\right)^2\right] = -\varphi_0\frac{4(x/h_i)}{[1-(x/h_i)^2]^2}. \tag{5}$$

4. Streamer triggering conditions

A developed streamer represents a long plasma channel which grows in an external electric field due to the generation of a strongly magnified electric field near its leading edge—the streamer tip. In a strong streamer tip field ionization of the ambient gas occurs. Being converted into plasma, the gas adds a new segment to the plasma channel. The charge of the streamer tip, which appears due to the open circuit current, serves as the source of the ionizing field. In the case of a positive streamer moving along the external field the streamer tip is charged positively due to electron outflow into the channel. Electrons from a newly ionized area are moved by the field filling the

'old' streamer tip, changing it into a new segment of the plasma channel, while the area previously occupied by those electrons becomes a new positively charged streamer tip. This process occurs continuously and has the nature of an ionization wave [5].

In order to generate a streamer in air the following three conditions have to be fulfilled.

1. The electric field must exceed the ionization threshold.
2. The initial plasma patch is sufficiently ionized so that the electric field generated by the space-charge, which is formed due to plasma polarization by the external field, is comparable with the external field itself. The space charge field should cancel the field inside the plasma patch and significantly increase the field at the leading front of the streamer in order to develop the ionization wave.
3. A seed of free electrons is required to start the ionization ahead of the streamer's front.

The latter condition is naturally fulfilled in the lower ionosphere, where a streamer develops in the preionized media. At the ground streamers produce initial electrons due to photoionization.

Let us consider a streamer initiated from a plasma sphere of radius R in an external field E_0. In order to expel the external field from the sphere, charges of different sign should be distributed on both hemispheres, with the surface charge density $q \sim \epsilon_0 E_0$ and total charge $eN_e \sim 2\pi R^2 q$. The exact solution for an ideal conducting sphere takes into account the nonuniform distribution of the surface charge. It gives [5]

$$eN_e = 3\epsilon_0 \pi R^2 E_0. \tag{6}$$

Therefore the minimum number of electrons in a plasma cloud which serves as a nucleus for the streamer is given by

$$N_{min} = \frac{3\epsilon_0 \pi R^2 E_{th}}{e} \tag{7}$$

where E_{th} is the electric field corresponding to the ionization threshold determined by a balance between the ionization of the air and dissociative attachment to molecular oxygen [12]. The latter condition means that ionization of the air has to occur in the magnified electric field outside the sphere. Moreover, the characteristic size of the sphere has to be higher than the ionization length α^{-1} in the space charge generating electric field, otherwise a sufficient number of electrons cannot be generated at a distance of the order R, where the above field drops to its initial value $E_0 \approx E_{th}$. Here α is the number of electrons generated on average by one electron in a unit path along the field.

The following analysis is based on the database developed for streamers observed under normal conditions and on similarity relations. A field of $E_0 = 31.4$ kV cm^{-1} causes a breakdown of an air gap of 1 cm at atmospheric pressure and produces an effective ionization coefficient $\alpha_{eff} = 12.4$ cm^{-1} [12]. Therefore from equations (6) and (7) one finds that at atmospheric pressure $R \sim \alpha^{-1} \sim 0.1$ cm, and $N_{min} \sim 2 \times 10^9$ electrons. The electron density required to initiate a streamer is $n_e \sim 3N_{min}/4\pi R^3 \sim 5 \times 10^{11}$ cm^{-3}. Since the value of the ionization threshold is proportional to the molecular density $E_{th} \sim N$, and $\alpha_{eff} \sim Nf(E/N)$, we obtain the following similarity relations

$$N_{min} \sim \frac{E_{th}}{\alpha_{eff}^2} \sim \frac{1}{N} \qquad R_{min} \sim \frac{1}{N} \qquad n_e \sim N^2. \tag{8}$$

Using (8) and the US Standard Atmosphere (1976), the minimum electron density in a plasma patch located at different heights required to develop a streamer was computed. In fact for altitude $h_i = 80$ km where $N = 4 \times 10^{14}$ cm^{-3} and $E_{th} \simeq 0.5$ V cm^{-1} the triggering conditions for a streamer require that $R_{min} \approx 60$ m, $n_e > 150$ cm^{-3}. The night-time ambient electron density is less than a few tens of electrons per cm^{-3} at 80 km. As revealed by previous estimates [9], such electron density patches can be generated at this altitude by EMPs from intracloud lightning.

5. Characteristics of a streamer tip

From the above discussion, the streamer when propagating downward enters much denser atmospheric layers. In addition, the longer the streamer channel becomes the larger the fraction of applied external potential drop across the channel—a role played by the voltage of the QS field from the thundercloud. This problem will be discussed in detail in the next section. Thus the characteristics of an ionization wave at the leading front of a streamer, such as velocity of the streamer v_s, density of electrons generated by the leading front of a streamer n_k, and radius of the streamer tip r_m, change as the front moves. We next find approximate relations for such characteristics using a simplified theory of streamer development in air [5] and similarity relations. In the next section these formulae will be used to develop boundary conditions for the developing streamer channel and to describe how the channel is growing. Figure 2 shows a schematic diagram of a streamer along with the distribution of the electron density n_e, longitudinal electric field E, and the 'spatial charge' density generated in this field, $\Delta n = n_+ - n_e$, where n_+ is the density of positive ions (density of the negative ions in the streamer tip is negligible).

Ionization occurring at the streamer front is described by the approximate equation

$$\frac{\mathrm{d}n_e}{\mathrm{d}t} = \nu_i(E) n_e \tag{9}$$

where ν_i is the effective ionization frequency determined by the difference between ionization and attachment rates. In the frame related to the streamer front moving with the speed v_s, equation (9) becomes

$$-v_s \frac{\mathrm{d}n_e}{\mathrm{d}x} = \nu_i n_e \qquad n_e(x) = n_0 \exp\left\{\frac{1}{v_s}\int_{-\infty}^{x} \nu_i \,\mathrm{d}x\right\} \tag{10}$$

where n_0 is the electron density ahead of the streamer tip. We consider for simplicity a 'strong' ionization wave propagating with a velocity v_s much higher than

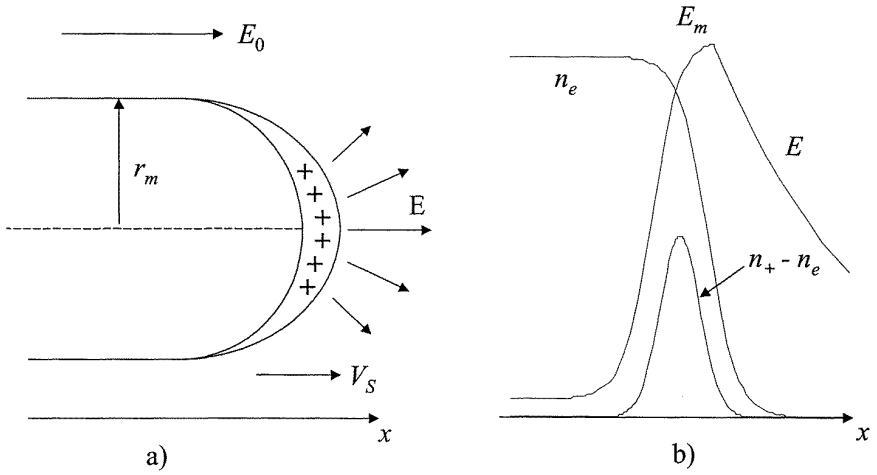

Figure 2. (a) Schematic diagram of streamer tip and the leading part of the channel. (b) The qualitative distribution of the electron density n_e, field E, and the difference between the densities of positive ions and electrons, which defines the density of space charge, along the streamer axis.

the electron drift velocity $v_e = \mu_e E$, where μ_e is the electron mobility. In the opposite case, an additional term appears in equation (10) when deriving it from the continuity equation; this term is negligible at $v_s \gg v_{e\,max}$ [5]. Since a strong field spreads ahead of the streamer tip at a distance of the order of its radius r_m (see figure 2) we obtain, from equation (10), the approximate relation for streamer velocity [13]

$$v_s \sim \frac{\nu_{im}\tau_m}{\ln(n_k/n_0)} \tag{11}$$

where $\nu_{im} \equiv \nu_i(E_m)$ and E_m is the maximum field corresponding to the leading edge of the streamer tip. Numerical coefficients of the order of unity which make equation (11) and the following formula (12) more accurate are given in [5, 14], along with the results of numerical integrations of more advanced equations for the ionization wave.

The electron density n_k behind the ionization wave, i.e. in the leading edge of the streamer channel, can be estimated based on the following considerations. Ionization ahead of the front serves as a preparation stage for the creation of a high-density plasma. Sufficient charge of the streamer tip, providing a strong ionizing field, is formed by this plasma. A few last generations of electrons, producing most of the subsequent electrons, are generated behind the ionization front in the region of space charge (see figure 2). Furthermore, the space charge exists over the relaxation time $\tau_r \approx \epsilon_0/en_k\mu_e$. Of the same order of magnitude is the characteristic time describing the dissipation of a strong field behind the ionization front. Thus a few last generations of electrons should be born during the time τ_r behind the front. This means that by an order of magnitude $\nu_{im}\tau_r \sim 1$, the density of electrons born in the ionization wave can be estimated by

$$n_k \sim \frac{\nu_{im}\epsilon_0}{e\mu_e} \sim \frac{\alpha(E_m)E_m\epsilon_0}{e} \tag{12}$$

where $\alpha = \nu_i/v_e = \nu_i/\mu_e E$ is the Townsend ionization coefficient.

Furthermore, two other characteristics, namely the radius r_m and maximum electric field E_m near the streamer tip still have to be obtained. These characteristics are related through the potential of the streamer tip. The electric field and potential of the streamer tip U are determined mostly by effects caused by space charge of the tip itself, and only partly by the space charge of the channel. The latter is concentrated near the channel surface. In fact, if the channel is an ideal conductor the charge becomes a surface charge. It can be shown [5] that in the case of perfectly conducting long cylinder with a semispherical tip, the input into the potential of the streamer tip is approximately the same from both components. In this case $U \approx 2E_m r_m$, while for a charged sphere $U = E_m r_m$. The streamer tip field reduces along the distance r_m ahead of the tip. In fact, $E(r) = E_m(r_m/r)^2$ for the case of a solitary charged sphere. However, in our case the QS electric field with potential U_0 exists in the space where the streamer tip is located. Therefore we obtain the following approximate relation for the values of r_m and E_m

$$U - U_0 \approx 2E_m r_m. \tag{13}$$

Here the potential of the tip, which describes the streamer 'strength', is an external characteristic relative to the tip itself. This potential presents a difference between the voltage inside the conducting channel with the electric current flowing along it, and the voltage of the external field across the streamer length.

The next problem deals with the values E_m and r_m established at the streamer front. As qualitatively discussed first by Cravath and Loeb [15] a self-regulating mechanism near the front of a growing plasma channel exists. In brief, if the radius r_m is too small and correspondingly the field E_m is too high, the propagating tip of the channel will rapidly expand under the action of a strong radial field. Thus the value of r_m increases following the reduction of the E_m. In the opposite case, when the radius r_m is high while the field E_m is low, any plasma bubble of a small radius of curvature which appears at the leading edge of

the ionization front could magnify the electric field pushing the ionization rate, and developing the plasma bubble, thus forming a channel of a smaller radius. Such an approach was used in [16] when formulating an approximate streamer theory. In this work a semi-qualitative criterion was introduced, helping to chose the value of E_m. According to [16] it corresponds to saturation or bending point of the dependence of the ionization frequency ν_i upon the field; the function $\nu_i(E)$ is steep at low E, then its growth reduces. More carefully chosen criteria for a proper choice of the value of E_m and the basic mechanism of self-regulation were considered recently [17] (see also [5], Appendix). In this work a quantitative relation between E_m and the function $\nu_i(E)$ and the electrostatic characteristics of the distribution of the charge space and the field along the streamer tip surface were found. Based on simplified numerical models of very long streamers [17] and on fairly accurate numerical models of short streamers [18–21] one can assume $E_m \approx 150$ kV cm^{-1} as the maximum streamer field under normal atmospheric conditions. This corresponds to $E_m/N \approx 6 \times 10^{-15}$ V cm^2 which will be used in the following model.

Therefore, based on the previous discussion, equations (11)–(13), similarity relations $E_m \sim N$, $\nu_{im} \sim \alpha_m \sim N$, $\mu_e \sim N^{-1}$, and taking into account the numerical model [14] of streamer propagation under normal atmospheric conditions, we introduce the following relations for the characteristics of a streamer tip moving in a nonuniform atmosphere

$$\begin{aligned} E_m &\approx 150(N/N_0) \text{ kV cm}^{-1} \\ r_m &\approx 0.1\left(\frac{U-U_0}{30 \text{ kV}}\right)(N/N_0) \text{ cm} \\ v_s &\approx 1.6 \times 10^8 \left(\frac{U-U_0}{30 \text{ kV}}\right) \text{ cm s}^{-1} \\ n_k &\approx 1.0 \times 10^{14}(N/N_0)^2 \text{ cm}^{-3} \end{aligned} \tag{14}$$

where $N_0 = 2.5 \times 10^{19}$ cm^{-3}. Here the value 30 kV is used for convenience; it should not be confused with the air breakdown threshold $E_{th} = 31.4$ kV cm^{-1}. These equations are valid for a strong ionization wave. As follows from the equations describing an ionization wave [5] when the streamer velocity and electron drift velocity at $E = E_m$ become comparable, the value v_s drops rapidly with the tip potential decreasing. Observations made under normal atmospheric conditions also indicate that the streamer velocity has a lower limit of the order of 10^7 cm s^{-1}, corresponding to drift velocity v_e. Therefore by studying streamer deceleration and the termination height we can extrapolate relations (14) up to $v_s \approx v_{e\,max} \approx 4 \times 10^7$ cm s^{-1}. The extrapolation brings about some inaccuracy when describing streamer propagation close to the stoppage point, which is a minor effect for our model. According to the similarity relations, $v_e \sim E/N$ and is independent of N if we can assume that the electron mobility does not depend on E. Thus we obtain that equation (14) are valid at $U - U_0 \geq 7.5$ kV and

$$v_s = 0 \text{ at } U - U_0 < 7.5 \text{ kV}. \tag{15}$$

Note that we neglected a small deviation from the similarity relations due to the logarithmic dependence of v_s on n_k in equation (11).

6. Initial electron density

We discuss next the origin of the initial electron density. In the lower ionosphere a sufficient ambient electron density exists, while in the stratosphere the initial electrons appear as a result of photoionization by a streamer tip. As shown in [5] by detailed calculations, under normal atmospheric conditions, photoionization provides the streamer with a sufficient number of initial electrons at the required distance from the tip. The value n_0, which affects the process only logarithmically, can be chosen from a wide range of values.

At high altitudes the air density drops and the conditions for the creation of initial electrons ahead of the streamer tip become more favourable. To explain this effect we consider the following simple model. The electron avalanche starts with photoelectrons of density n_0 at a certain distance r_0 from the centre of the streamer tip along its axis. The coordinate r_0 is approximately estimated from the condition that along the whole distance from r_0 to infinity a single generation of electrons can be produced due to the impact ionization [5]. Furthermore, r_0 is a few times higher than the radius r_m of the streamer tip, and it depends logarithmically upon the ratio n_k/n_0. In order to start the electron avalanche at the point r_0, at least one photoelectron has to be presented inside, say, a cylindrical volume extended along the streamer tip axis, having radius r_m and length δ, along which a single generation of electrons is produced. The length δ is a few times less than r_0 [5] and, like r_0, it is proportional to r_m. Therefore taking into account the similarity relations (14) $r_m \sim N^{-1}$, the minimum initial density of the photoelectrons at the distance r_0 from the streamer tip is proportional to

$$n_{0\,min} \sim 1/\pi r_m^2 \delta \sim N^3. \tag{16}$$

Let us now estimate the number of photoelectrons created. The density of air molecules excited due to the electron avalanche is proportional to the electron density inside the streamer tip n_k. Unlike the process occurring under normal atmospheric conditions at high altitude, where $r_m \sim N^{-1}$ is high enough, excited molecules having a short lifetime τ^* have radiated before the streamer tip moves out, since $v_s\tau^* \ll r_m (v_s \sim 10^8$ cm s^{-1}, $\tau^* \sim 10^{-8}$ s, $r_m \gg 1$ cm). Thus the total amount of the excited molecules inside a streamer tip of volume Z^* is proportional to

$$Z^* \sim n_k \pi r_m^2 v_s \tau^* \tag{17}$$

while the power of the photon source

$$F = Z^*/\tau^* \sim n_k \pi r_m^2 v_s. \tag{18}$$

The photoelectron density produced at a distance r_0 from such a source is proportional to

$$n_0 \sim \frac{F\chi \exp(-\chi r_0)}{4\pi r_0^2}\left(\frac{r_0}{v_s}\right) \sim n_k \left(\frac{r_m}{r_0}\right)^2 (\chi r_0)\exp(-\chi r_0) \tag{19}$$

where χ is the absorption coefficient of the ionizing emission, which for the sake of simplicity we assumed monochromatic and r_0/v_s is the timescale of photoelectron accumulation in a given location. According to the similarity relations (14) $n_k \sim N^2$, $\chi \sim N$ and $r_0 \sim N^{-1}$, thus the actual initial electron density $n_0 \sim N^2$ drops with attitude slower than the minimum density required to produce a streamer $n_{0min} \sim N^3$. If the emission is non-monochromatic and χ depend sharply on frequency [5], the situation becomes even more favourable at higher altitudes, namely $n_0 \sim N$. Thus since a streamer provides itself with enough initial electrons under normal atmospheric conditions, at high altitudes it can be done easily.

7. Equations describing streamer growth

As shown in [5] the longitudinal field at the beginning of a streamer channel just behind the ionization wave is

$$E_k \approx \frac{2E_m}{\ln(l/r_m)\ln(n_k/n_0)} \tag{20}$$

where l is the streamer length. For a long streamer the above field is two orders of magnitude weaker than the maximum E_m. Neither ionization nor dissociative attachment takes place in a such weak field. Electrons are removed from the streamer channel by three-body attachment to O_2, and by electron–ion recombination. However, the plasma decay is less important for streamer development in the upper atmosphere than in a dense air, where it controls the whole process.

At values of the E/N ratio which take place in the streamer channel the mean electron energy $\bar{\varepsilon} \approx 0.8$–$1.2$ eV, and the rate constant of three-body electron attachment to molecular oxygen is 5×10^{-31} cm^6 s^{-1} (the role of a third body is played by O_2, while N_2 plays only a minor role) [22]. Thus the characteristic attachment time is $\tau_{att} = 5 \times 10^{31} N^{-2}$ s. The characteristic electron–ion recombination time behind the streamer tip $\tau_{rec} = (\beta n_k)^{-1}$. Taking into account that according to equation (14) the electron density in the tip $n_k \approx 1.6 \times 10^{-25} N^2$ cm^{-3}, while the recombination coefficient at such electron energy $\beta \approx 10^{-7}$ cm^3 s^{-1}, we obtain that $\tau_{rec} \approx 6.2 \times 10^{31} N^{-2}$ s. Electron decay intensifies strongly at lower altitudes, however. Even at the lowest altitude reached by the streamer $h \simeq 50$ km, $N = 2.1 \times 10^{16}$ cm^{-3}, $\tau_{att} \approx 0.11$ s and $\tau_{rec} \approx 0.14$ s. This is an order of magnitude higher than the propagation time of the streamer. Note that plasma in the streamer channel starts to decay only after termination of the streamer growth, so when considering streamer growth, plasma decay can be neglected. In this case the resistance of a unit length of the channel, which is given by

$$R_1 = (\pi r_m^2 e \mu_e n_k)^{-1} \tag{21}$$

does not change with time and is determined by the values of r_m and n_k produced by the ionization wave at a certain location x where the air density is $N(x)$. The coordinate x is counted downward from the region where the streamer was initiated.

The channel expands very slowly due to ambipolar diffusion and the expansion does not change the resistance since the number of electrons per unit length of the channel $\sim(\pi r_m^2 n_k)^{-1}$ remains constant. Therefore this effect can be neglected.

The distributions of potential $U(x,t)$ and current $I(x,t)$ along the streamer channel, which determine the potential of the streamer tip U_l as well as the streamer velocity v_s, are approximately described by the equations of a long line with the distributed characteristics. Neglecting self-induction, as justified by the estimates reported in [5], the equations have the following form

$$\begin{aligned} \frac{\partial q}{\partial t} + \frac{\partial I}{\partial x} &= 0 \\ \frac{\partial U}{\partial x} &= -I R_1 \\ q &= C_1(U - U_0) \end{aligned} \tag{22}$$

where q and C_1 are the charge and capacity per unit length of the channel. The latter can be considered as independent of x and equal to the mean capacity per unit length (in F cm^{-1}) of a long thin conductor

$$C_1 = \frac{2\pi\epsilon_0}{\ln(l/r)} = \frac{0.55 \times 10^{-12}}{\ln(l/r)}. \tag{23}$$

Since C_1 depends only logarithmically on both r and l, the radius of the channel tip at given t can be substituted into equation (23).

We next formulate the boundary and initial conditions for equations (22). The potential U is equal to the external potential U_0 at the altitude $x = 0$ where the streamer is initiated. Above this altitude the ionosphere can be considered as a perfect conductor, so the electric field does not penetrate it. The external potential is counted from this boundary, thus

$$U(x=0) = U_0(x=0) = 0. \tag{24}$$

The conducting current is not closed at the channel tip where $x = l$ and $I = I_l$. This current is spent to deliver charge to the segment of the channel acquired over unit time. Taking equations (22) into account we obtain

$$I_l(x=l) = q_l v_s = C_1(U_l - U_0)v_s(l) \tag{25}$$

where $U_l \equiv U(x = l)$. According to equations (14), obtained by analysing the process in the streamer tip, v_s is a function of the potential difference $U_l - U_0$. Furthermore, the streamer growth is defined by

$$\mathrm{d}l/\mathrm{d}t = v_s. \tag{26}$$

Therefore the characteristics of the streamer channel and tip are coupled by equations (14), with U_l instead of U and equations (21)–(26). Such an approach can describe the development of a streamer. Initially a streamer of small length l_0 with the given characteristics is considered. One can assume for simplicity that the potential along the initial streamer is constant, $U = 0$, as for a perfect conductor. In this case the initial velocity will be defined

by the tip potential $U - U_0(l_0) = -U_0(l_0) = |U_0(l_0)|$. The resistance R_1 inside the initial channel can be considered as corresponding to this potential. The computations can be terminated when the voltage $U_l - U_0$ falls below 7.5 kV which corresponds to v_s close to the maximum electron drift velocity.

From the above equations and boundary conditions the charge conservation relation follows automatically:

$$I(0,t) = \frac{\mathrm{d}}{\mathrm{d}t}\int_0^l q(x,t)\,\mathrm{d}x. \qquad (27)$$

It can be applied to control the numerical computations.

8. Results of the computations and discussion

In order to conduct a numerical integration it is convenient to reduce the equation set (22) to a single nonlinear equation for $U(x,t)$. This is a parabolic type equation which describes nonlinear diffusion of the potential. The role of the diffusion coefficient is played by the inverse resistance per unit length R_1^{-1}. The boundary condition (25) relates $\partial U/\partial x$ and U at $x = l$, after exclusion of I.

When conducting the integration the spatial step was taken to be constant. The time step was variable, in fact we chose $\Delta t = \Delta x/v_s[l(t)]$. Thus the channel lengthens by Δx at any time step. The absolutely stable algorithm was applied in order to solve the nonstationary equation for $U(x,t)$ at any time step by using the implicit scheme of the Crank–Nicholson type of second-order accuracy. A standard method of trigonal inversion (see, for example, [23]) was used. At the initial moment the streamer had length $l_0 = 0.2$ km; $|U_0(l_0)| \approx 0.2$ kV was assigned. The step Δx was chosen such that when it reduced by an order of magnitude, solution of the equation changed by less than 1%. The results below were obtained using the step $\Delta x = 0.3$ km, i.e. at a later stage when $l \approx 30$ km, the streamer channel was divided by 100 segments, which provided good accuracy. The density of the standard atmosphere was approximated by

$$N = 4.03\times10^{14}\exp[(80-h)/\Delta_0]\ \mathrm{cm}^{-3} \qquad \Delta_0 = 7.23\ \mathrm{km} \qquad (28)$$

in the altitude range $h \approx 50$–80 km. Results of the computations are shown in figures 3 and 4. The streamer launching downward from the ionosphere accelerates first, then slows down, and finally stops. The maximum velocity $v_s \approx 1.2\times10^9$ cm s^{-1} is reached in 4 ms, and the streamer growth is terminated in about 6.7 ms. This happens at the altitude $h_{stop} \approx 48$ km, thus the streamer propagates along the distance $l_{max} \approx 32$ km, leaving behind a plasma trail in the altitude range 80–48 km above ground. This is consistent with the observations of red sprites. According to equations (12) and (14), the plasma density produced by the streamer increases in the downward direction proportionally to the square of the air density. The growing time of the streamer is 7 ms, i.e. an order of magnitude less than the characteristic times of electron attachment and recombination. This justifies neglect of the plasma decay in our model.

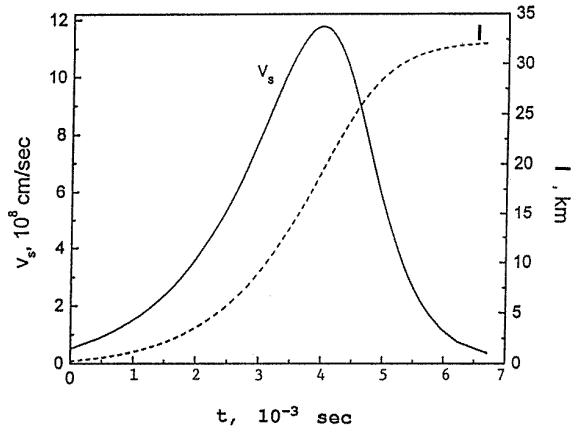

Figure 3. Dependence of the streamer velocity and length on time, computed for a nonuniform atmosphere.

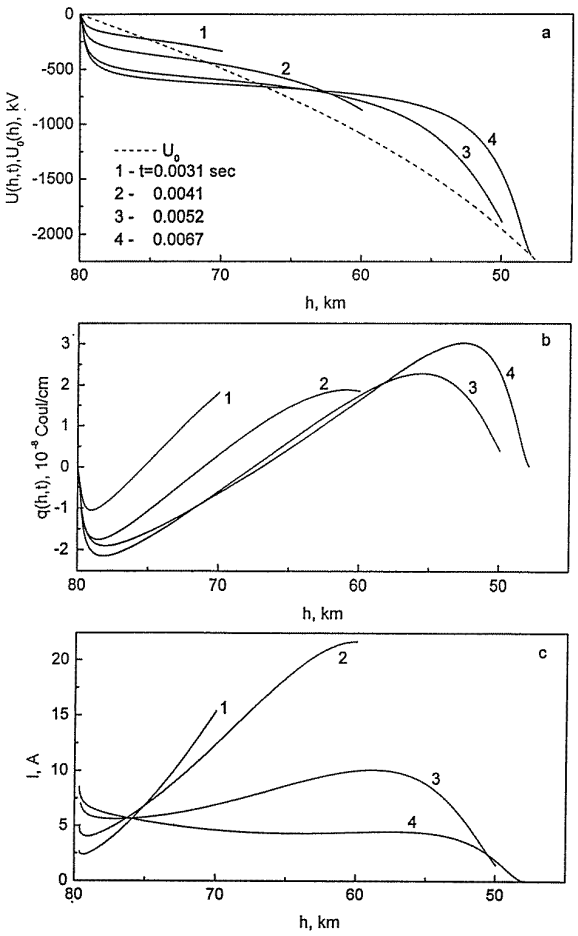

Figure 4. (a) Distribution of the potential, (b) charge per unit length, and (c) the current along the streamer channel computed for a few consecutive times shown in the figure, under the same conditions as figure 3.

The development of the streamer resembles that occurring in the laboratory experiments where streamers, as a rule, are launched from a small high-voltage electrode (mostly positive). They then move toward a large grounded electrode in a sharply reducing external field.

In our case both 'electrodes' (ionosphere as the anode and negatively charged thundercloud as the cathode) have a significant horizontal extent. Thus the nonuniformity rate of the external field is less than that in the laboratory. Furthermore, while in the laboratory the streamer moves in the direction of the field reduction, in our case it moves toward the charged cloud entering an increasingly intense field. However, the discharge processes involving a weakly ionized plasma are affected not by the field E, but by the ratio E/N which decreases strongly in the direction of streamer propagation due to the increasing air density. This makes the discussed process similar to laboratory experiments.

The 'laboratory' streamers also first accelerate, then slow down, and finally stop. The maximum streamer velocity of about 10^9 cm s^{-1} found by our computations is typical for laboratory streamers under a voltage of a few hundreds of kilovolts. As found by numerous experiments [5] a streamer cannot cross a discharge gap of length d if the voltage applied to the anode U_a is such that a mean field in the gap $E_m = U_a/d$ is less than the critical field E_{cr}. The latter depends on the type of gas and the gas density. In air under normal conditions $E_{cr} \approx 4.5$–5 kV cm^{-1}. In gases with no electron attachment, the value of E_{cr} is a few times less than that. In fact, in nitrogen at $P = 1$ atm, $E_{cr} \approx 1.5$ kV cm^{-1}, which corresponds to $E_{cr}/N = 6 \times 10^{-17}$ V cm^2.

Under extreme conditions when the streamer barely crosses a long discharge gap, it reaches the electrode with an extremely low velocity. The potential of the tip slightly exceeds the local external potential. Practically, the overall applied high voltage U_a falls across the streamer channel, i.e. E_{cr} is ultimately averaged field in the long streamer channel just before its stop. Thus this value can be used in order to evaluate the maximum length of the streamer even in such cases when it stops without crossing the discharge gap: $l_{max} \approx \Delta U/E_{cr}$, where ΔU is the external voltage drop across the length l_{max}.

We now generalize this empirical criterion for the inhomogeneous atmosphere. Bearing in mind that the controlling role is played by the ratio E/N rather than by E, we introduce concepts of $(E/N)_{av}$ and $(E/N)_{cr}$. The average E/N value yields the following equations

$$\Delta U = |U_0(l)| = \int_0^l \frac{E}{N} N \,\mathrm{d}x = \left(\frac{E}{N}\right)_{av} \int_0^l N \,\mathrm{d}x$$
$$= \left(\frac{E}{N}\right)_{av} N(h_i - l)\Delta_0 \qquad (29)$$

where the integral is computed using equation (23), and $N(h_i - l)$ is the air density at the altitude $h_i - l$ reached by the streamer tip. The altitude where the streamer stops, h_{stop} is obtained from the equation

$$N(h_{stop}) \approx |U_0(l_{max})|/\Delta_0 (E/N)_{cr} \qquad l_{max} = h_i - h_{stop}. \qquad (30)$$

If we substitute the values $l_{max} = 32$ km, $h_{stop} = 48$ km, ($N(h_{stop}) = 4 \times 10^{16}$ cm^{-3}), $|U_0(l_{max})| \approx 2000$ kV into this equation, we find that $(E/N)_{cr} = 7 \times 10^{-17}$ V cm^2, which is close to the results of the laboratory experiments using nitrogen, 6×10^{-17} V cm^2. Note that the discussed situation is closer to the streamer in nitrogen, since electron attachment is not important in our case. A similar result was obtained by computing streamer growth in a gas without electron losses, under the normal atmospheric density N_0, using equations (14) and (21)–(26). The streamer launched from a spherical anode of the radius 5 cm, to which a voltage $U = 500$ kV was applied, rapidly reached a speed of 1.3×10^9 cm s^{-1}, then started to slow down, and stopped over 1 μs, travelling the distance $l_{max} \approx 3.2$ m. The critical value $(E/N)_{cr}$ was the same as above: $(E/N)_{cr} = U/(N_0 l_{max}) = 6.2 \times 10^{-17}$ V cm^2.

However, let us not overestimate the close coincidence of the computations with the experiment. Recombination occurring in nitrogen under atmospheric pressure was not taken into consideration in the computations. The resulting plasma decay leads to an increase of E_{cr}. In fact, computations made by taking into account the recombination, give $l_{max} \approx 1.1$ m, i.e. three times the increase of E_{cr}. The fact that the model agrees with the experiment within an order of magnitude, however, indicates the sufficiency of the model.

As seen from figure 4 the streamer channel is strongly polarized by the external field. The charge is pumped in the leading part of the channel from the ionosphere, as described by equation (27), and from the rear part of the channel. The latter has a negative charge and its potential drops below the external $U_0(x)$. This does not happen when the streamer grows in the rapidly falling field of a small electrode of high voltage. Such a situation is typical for the case when the streamer grows from the middle of the discharge gap toward both of the electrodes in a constant external field, and it is not linked to any of the electrodes. Our case is different from those observed in the laboratory by much higher values of the E/N ratio for the external field, which produces strong polarization inside the conducting channel, despite the fact that the channel is connected with the electrode or 'ionosphere'. Charge transfer from the rear part of the channel to its leading part corresponds to the rise of the current toward the streamer tip (see figure 4). At a later stage of the process the current in the leading part of the channel is reduced when close to the tip due to a strong increase of the resistance, since $R_1 \sim N$, in agreement with equations (14) and (21).

A sharp reduction of the velocity of the decelerating streamer is caused by a decrease of the current which feeds up the tip. In our computations the moment when the current stops is formally described by the condition (15), which approximately reflects a sharp reduction of the streamer velocity, when it becomes comparable to the electron drift velocity in the maximum field of the streamer tip. However, even if one is not pushing the streamer to a stop by applying equation (15), but instead continues the computations by extrapolating equations (14) in the range $U - U_0 < 7.5$ kV, $v_s < v_{e\,max} \approx 4 \times 10^7$ cm s^{-1}, the streamer velocity continues to drop and it propagates over a small additional distance. This is due to a steady increase of the air density N and resistance R_1 of the newly added segments of the channel. In a longer slow down, electron decay in the channel becomes

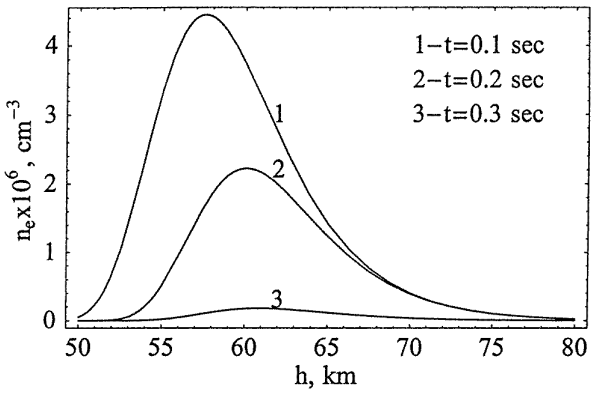

Figure 5. Vertical distribution of electron density in the streamer trail.

important and therefore the resistance of the whole channel increases, leading to termination of the streamer growth. Thus the stopping altitude of the streamer has a weak sensitivity to the initial assumptions and premises of the theory. We also checked that the value of h_{stop} is not sensitive to variations of the parameters of equations (14) and (15) describing the streamer tip. The streamer channel mostly narrows in the downward direction. At an altitude of 60 km its radius is about 40 m according to equation (14).

After termination of the streamer development the plasma generated by the streamer decays in accordance with the kinetic equation

$$\frac{\mathrm{d}n_e}{\mathrm{d}t} = -\frac{n_e}{\tau_{att}} - \beta n_e^2 \qquad n_e(x,0) = n_k(x) \tag{31}$$

where β and n_k were discussed in section 7. In the streamer trail, where the electric field is weak, the electrons are thermalized reaching a mean energy $\bar{\varepsilon} \approx 0.02$–$0.03$ eV, correspondingly $\tau_{att} \approx 8.85 \times 10^{30}\ N^{-2}$ s (the attachment rate constants are 2×10^{-30} cm^6 s^{-1} and 1.5×10^{-31} cm^6 s^{-1} for O_2 and N_2 as a third body respectively [24]). Equation (31) yields the following solution

$$n_e(x,t) = \frac{n_k(x)\exp(-t/\tau_{att})}{1 + \beta n_k(x)\tau_{att}[1 - \exp(-t/\tau_{att})]}. \tag{32}$$

Since $n_k \sim N^2$, while $\tau_{att} \sim N^{-2}$, the plasma density reduction with altitude smoothens over time, as illustrated by figure 5. This figure shows the altitude distribution of the electron density in the streamer trail 0.1, 0.2 and 0.3 s after plasma generation. We recall that the streamer stops in 0.007 s, therefore the initial moments of plasma decay can be considered as independent of x.

9. Conclusions

It has been suggested that the optical flashes observed above giant thunderstorms at altitudes of 50–90 km, termed red sprites, are caused by streamers. They propagate downward from the lower ionosphere in the quasistatic electric field left in the ionosphere following lightning discharge. The streamers are nucleated by plasma patches generated in the lower ionosphere by electromagnetic pulses from horizontal intracloud lightning.

In order to check this hypothesis we developed a theory and conducted some numerical simulations considering a single streamer propagating in a nonuniform atmosphere in a field induced by a charged cloud. According to our computations a streamer starting at 80 km above ground propagates downward to an altitude of 48 km; the propagation time is about 7 ms. These results are consistent with observations [4]. As a result a plasma channel of varying cross section is formed, having a maximum diameter of about 100 m, and an increasing downward electron density which is proportional to the square of the neutral density. Later the plasma starts to decay. We suggest that the emission of this plasma has been observed.

The discussed model of a single streamer represents a first important step in streamer studies. In reality a number of streamers, similar to what happens in streamer corona, occur. In this process electrostatic interaction and branching of different charged plasma channels could be substantial. Studies of multiple streamers in the upper atmosphere present a much more complicated problem, and we will investigate this at the next stage. Analysis of optical emissions of the streamer plasma is also needed in order to obtain their intensity, spectra and duration. The model can then be compared with existing observations. We hope that these studies will yield a better understanding of the nature of red sprites, which not only present interesting basic science but could be important for future aeronautics problems. The simple models of streamer development presented in this paper could be applied as a tool for operative calculations in studies of laboratory streamers.

Acknowledgments

This work was supported by NSF grant ATM 9422594. We also express our gratitude to K Papadopoulos and J A Valdivia for helpful discussions.

References

[1] Sentman D D, Wescott E M, Osborne D L, Hampton D L and Heavner M J 1995 Preliminary results from the sprites94 aircraft campaign: red sprites *Geophys. Res. Lett.* **22** 1205–8

[2] Lyons W A 1996 Sprite observations above the U.S. High Plains in relation to their parent thunderstorm systems *J. Geophys. Res.* D **101** 29 641–55

[3] Winckler J R, Lyons W A, Nelson T E and Nemzek R J 1996 New high-resolution ground-based studies of sprites *J. Geophys. Res.* D **101** 6997–7004

[4] Cummer S A and Inan U S 1997 Measurement of charge transfer in sprite-producing lightning using ELF radio atmospherics *Geophys. Res. Lett.* **24** 1731–4

[5] Bazelyan E M and Raizer Yu P 1997 *Spark Discharge* (Boca Raton, FL: CRC)

[6] Milikh G M, Papadopoulos K and Chang C L 1995 On the physics of high altitude lightning *Geophys. Res. Lett.* **22** 85–8

[7] Fernsler R F and Rowland H R 1996 Models of lightning-produced sprites and elves *J. Geophys. Res.* D **101** 29 653–59

[8] Pasko V P, Inan U S and Bell T 1996 Sprites as luminous columns of ionization produced by quasi-electrostatic thundercloud fields *Geophys. Res. Lett.* **23** 649–52
[9] Valdivia J A, Milikh G M and Papadopoulos K 1997 Red Sprites: lightning as a fractal antenna *Geophys. Res. Lett.* **24** 3169–72
[10] Le Vine D M and Meneghini R 1978 Simulations of radiation from lightning return strokes: the effects of tortuosity *Radio Sci.* **13** 801–12
[11] Williams E R 1988 The electrification of thunderstorms *Sci. Amer*. 88–99
[12] Raizer Yu P 1991 *Gas Discharge Physics* (Berlin: Springer)
[13] Loeb L B 1965 Ionizing wave of potential gradient *Science* **148** 1417–26
[14] Raizer Yu P and Simakov A N 1996 Semispherical model of a streamer head *Plasma Phys. Rep.* **22** 603–7
[15] Cravath A M and Loeb L B 1935 The mechanism of the high velocity of propagation of lightning discharges *Physics* **6** 125–7
[16] D'yakonov M I and Kachorovskii V Yu 1991 Stationary propagation of streamers in electroactive gases *Sov. Phys.–JETP* **71** 498–505
[17] Raizer Yu P and Simakov A N 1998 What does define the radius and maximum field near the long streamer tip? *Plasma Phys. Rep.* **24** (N8)
[18] Vitello P A, Penetrante B M and Bardsley J N 1994 Simulation of negative-streamer dynamics in nitrogen *Phys. Rev.* E **49** 5574–98
[19] Babaeva N Yu and Naidis G V 1997 Two-dimensional modeling of positive streamer dynamics in non-uniform electric field in air *J. Phys. D: Appl. Phys.* **29** 2423–31
[20] Kulikovsky A A 1997 Positive streamer between parallel plate electrodes in the atmospheric pressure air *J. Phys. D: Appl. Phys.* **30** 441–50
[21] Morrow R and Lowke J J 1997 Streamer propagation in air *J. Phys. D: Appl. Phys.* **30** 614–27
[22] Schneider B I and Brau C A 1982 Two- and three-body electron attachment in air *J. Phys. B: At. Mol. Phys.* **15** 1601–7
[23] Andeson D, Tannehill J and Pletcher R 1984 *Computational fluid mechanics and heat transfer* (New York: Hemisphere)
[24] Christophorou L G 1984 *Electron–Molecule Interactions and Their Applications* (Orlando: Academic)